Dynamics of strongly dissipative systems

H. P. Fang
*China Center of Advanced Science and Technology (World Laboratory), P.O. Box 8730, Beijing 100080, China and Institute of Theoretical Physics, P.O. Box 2735, Beijing 100080, China**

(Received 6 January 1994)

The attractors in two-dimensional (2D) phase space of the strongly dissipative Hénon map are reduced to those of an effectively 1D map. From the grammar for this effectively 1D map we can generate all of the unstable periodic orbits, which are exactly consistent with those from the 2D map obtained directly both with a Newton procedure and the techniques of Biham and Wenzel [Phys. Rev. Lett. **63**, 819 (1989)]. This idea provides a method to give a very precise and not too cumbersome estimate of the characteristic quantities of strange attractors of strongly dissipative systems. It is also helpful to understand many observations on high-dimensional systems both experimentally and numerically.

PACS number(s): 05.45.+b

I. INTRODUCTION

Dissipative nonlinear dynamical systems have received a great deal of attention in the last thirty years. Some of them possess very strong dissipation. Take the Hénon map [1]

$$x_{n+1} = 1 - ax_n^2 + y_n, \qquad y_{n+1} = bx_n. \tag{1}$$

as an example. In the equations, a and b are both parameters. The Jacobian of this map is

$$J = \begin{bmatrix} -2ax_n & 1 \\ b & 0 \end{bmatrix}. \tag{2}$$

When the determinant $|J| = b = 1$, it preserves the area and thus imitates a conservative dynamical process. In the extreme dissipative limit, $b = 0$, it reduces to the 1D logistic map

$$x_{n+1} = 1 - \mu x_n^2. \tag{3}$$

In the case of $b << 1$, the strong contraction of the area may be thought to be due to the presence of very strong dissipation. For these strongly dissipative systems, on one hand, the strange attractors clearly indicate that the maps are two dimensional. In Fig. 1 the strange attractor of the Hénon map for $a = 1.4$ and $b = 0.05$ is shown, which has a clear hook in the upper-left part of the solid line. On the other hand, numerical and experimental investigations have already shown that the periodic orbits of some high-dimensional systems share universal features with those of one-dimensional (1D) maps [2–9]. In 1988, Gunaratne, Jensen, and Procaccia [2] claimed that for maps of the annulus of the family

$$\theta_{n+1} = \theta_n + \Omega + f(\theta_n) + bh(r_n), \text{ mod } 1, \qquad r_{n+1} = bh(r_n) + f(\theta_n) \tag{4}$$

there exists a value b_c of b, such that for $b < b_c$ the topology is identical to that of the 1D circle map at least on numerical grounds. For some ordinary differential equations, it is found that the systematics of the periodic windows can be represented by 1D maps rather well (the Lorenz equations [3], the Duffing equations [4], the forced Brusselator [5], the Rössler's band [6], and the double-diffusive convection system [7], etc.). The most striking and detailed observation is obtained in the Lorenz equations. For most of the parameters, the at-

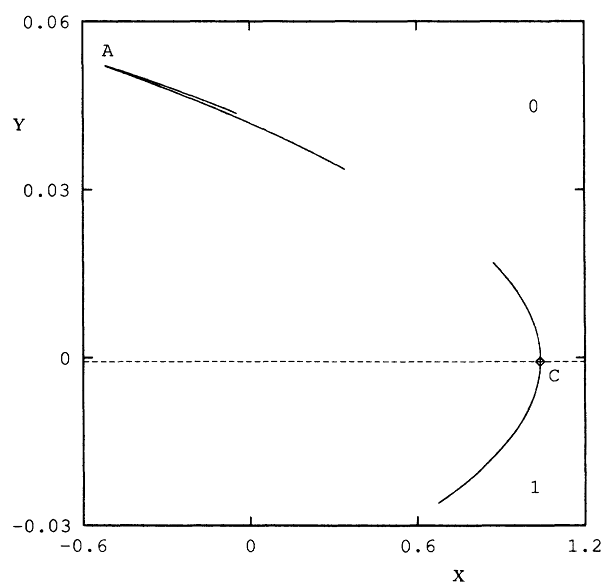

FIG. 1. The strange attractor of the Hénon map for (a, b) = (1.4, 0.05). The heavy lines are the strange attractor. The diamonds are the "primary" tangencies. The dashed line connecting them divides the full attractor into two subsets marked by 0 and 1.

*Address for correspondence.

TABLE I. The kneading sequences and fractal dimensions for the Hénon map for different parameters. The last column lists the μ values for the logistic map (3) for corresopnding kneading sequences.

a	b	K_f	Dimension	μ
1.4	0.05	0100010100010100010100010101010001	1.05 ± 0.01	1.4715
1.7	0.01	0100100001001010100010101	1.14 ± 0.03	1.70856

tractors on the proper 2D Poincáre sections are almost topologically equal to those of a 1D antisymmetrical map. Experimentally, even though the Belousov-Zhabotinskii reaction involves more than thirty chemical species, it exhibits rather complex behavior that is modeled well by 1D maps [9]. These observations motivate our interest in discussing the relation between these strongly dissipative systems and their extreme dissipative counterparts. In this paper, we take the Hénon map as an example. It is found that the chaotic dynamics of the Hénon map (1) with parameters $b << 1$ is so close to a 1D map that it can be treated as a 1D map with a proper parameter. The proper parameter is determined by a and b in the Hénon map (see Table I).

The paper is organized as follows. In Sec. II, we review the basic properties of 1D unimodal maps and 2D Hénon map. A technique called symbolic dynamics is used. The dynamics for the strongly dissipative Hénon map is studied in Sec. III. To demonstration the validity of the method presented in Sec. III, the Rössler equations is investigated in Sec. IV. Finally, in Sec. V we give our conclusion.

II. BASIC PROPERTIES OF 1D UNIMODAL MAPS AND HÉNON MAP

To study the chaotic dynamics of a dynamical system, it is widely accepted that a most useful way is to consider the set of unstable periodic orbits embedded in them [10, 11]. It was shown that characteristic quantities of strange attractors like Lyapunov exponents, entropies, dimensions, and $f(\alpha)$ spectra can be directly related to properties of unstable periodic orbits. Until recently, symbolic dynamics provides the most robust technique for the calculation and classification of unstable periodic orbits in a dynamical system [11–15].

To construct the symbolic dynamics of a dynamical system, the determination of the partition and the ordering rules for the underling symbolic sequences is of crucial importance. In the case of 1D maps, the partition is just the set of the critical points. For example, for unimodal maps, a binary generating partition divides the interval into two branches lying to the left and right of the maximum, respectively. The right branch is assigned 0, whereas the left branch is assigned 1. As a consequence, nearly all trajectories are unambiguously encoded by infinite strings of bits $S(x) = (s_0 s_1 s_2 \cdots)$, where s_i is either 0 or 1 for unimodal maps [13]. As a matter of fact, the ordering rules for these symbolic strings can be deduced from the natural order of the number on a 1D interval. Analytically, these ordering rules correspond to the ordering for the following "forward" variables

$$\alpha(\mathrm{S}(x)) = \sum_{i=0}^{\infty} \mu_i 2^{-(i+1)}, \tag{5}$$

with

$$\mu_i = \begin{cases} 0 \text{ for } \sum_{j=0}^{i}(1-s_i) = 0, & \text{mod } 2 \\ 1 \text{ for } \sum_{j=0}^{i}(1-s_i) = 1, & \text{mod } 2. \end{cases} \tag{6}$$

After the kneading sequence K (i.e., the forward symbol sequence from the maximum) is determined and $\alpha(K)$ is calculated, from the above ordering rules the grammar for a word allowed or forbidden is obtained, which is: a word $S(x)$ corresponds to a real trajectory if and only if it satisfies

$$\alpha(\sigma^m(\mathrm{S}(x))) \leq \alpha(K), \quad m = 0, 1, 2, \ldots, \tag{7}$$

where σ denotes the shift operator. Consequently, the characteristic quantities of strange attractors of the map for given parameters are completely determined.

For 2D maps, if one wants to split the full phase space into parts, 1D curves should be introduced, which are called partition lines. For the Hénon map, it has been verified that a binary generating partition is convenient, which is the set of all "primary" tangencies between stable and unstable manifolds [12]. Analogously, letters 0 and 1 are assigned for different parts. For the Hénon map, x_i depends not only on x_{i-1}, but also on x_{i-2} so that the backward sequences have to be considered. All trajectories are then encoded by double-infinite strings of bits $S(x) = \ldots s_{\bar{m}} \ldots s_{\bar{1}} s_{\bar{0}} \bullet s_0 s_1 s_2 \ldots s_n \ldots$, where s_n denotes the letter for nth image, $s_{\bar{m}}$ the letter for the $\bar{m}$th preimage, each is either 0 or 1, the solid dot indicates the "present" position. In order to extend the admissibility conditions for the unimodal maps to this map, it is convenient to introduce a "backward" variable defined as

$$\beta(S(x)) = \sum_{\bar{i}=0}^{\infty} \nu_i 2^{-(\bar{i}+1)}, \tag{8}$$

with

$$\nu_i = \begin{cases} 0 \text{ for } \sum_{j=0}^{\bar{i}} s_j = 1, & \text{mod } 2 \\ 1 \text{ for } \sum_{j=0}^{\bar{i}} s_j = 0, & \text{mod } 2. \end{cases}$$

For this 2D map, each primary tangency C associates a double-infinite kneading sequence K (with the first backward letter $s_{\bar{0}}$ undetermined which may be 0 or 1) and two symmetrical points $(\alpha(K), \beta_-(K))$ and $(\alpha(K), \beta_+(K) = 1 - \beta_-(K))$ in the symbolic plane corresponding to $s_{\bar{0}} = 0$ and 1, respectively [14]. Analogously to those in the unimodal maps, for all allowed points (α, β) with $\beta \in [\beta_-(K), \beta_+(K)]$, α should be less than $\alpha(K)$ and thus the pruning front is obtained by cutting out rectangles $\{\alpha, \beta | \alpha > \alpha(K), \beta \in [\beta_-(K), \beta_+(K)]\}$ for all P. The union of these rectangles gives the fundamentally forbidden zone. Consequently, the grammar for a word allowed or forbidden in this map can be expressed as: A double-infinite word is admissible if and only if all its shifts never fall into the fundamentally forbidden zone [14]. It is clear that there are infinite kneading sequences (corresponds to infinite primary tangencies) in a 2D map to determine the grammar for a word allowed or forbidden, while there is only one kneading sequence in a 1D map.

III. THE DYNAMICS OF STRONGLY DISSIPATIVE HÉNON MAP

In this section, we concentrate on the strongly dissipative Hénon map. We find that the topology of the attractors of the Hénon map are so close to 1D that they can be treated as that of a 1D map when the dissipation is strong enough (b is sufficiently small). In Fig. 1, the strange attractor for $(a, b) = (1.4, 0.05)$ is shown. The hook clearly reveals that the map is two dimensional. In the following, we will show that the periodic orbits embedded in these chaotic attractors can be precisely determined with only one kneading sequence as in 1D maps.

We first construct the symbolic dynamics for the Hénon map for $(a, b) = (1.4, 0.05)$. The primary tangency points (diamonds) are also shown in Fig. 1. Twenty primary tangency points are found and the kneading sequences are computed. The symbolic plane is shown in Fig. 2 where dots represent real orbits. It is remarkable to find that all the forward parts of these kneading

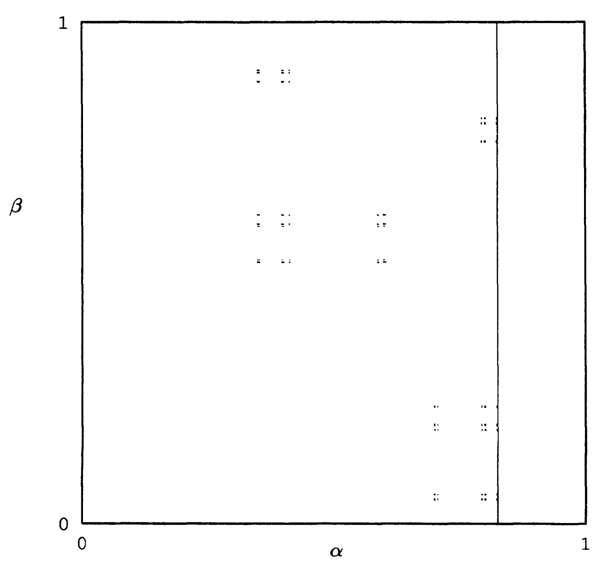

FIG. 2. The symbolic plane of the Hénon map for (a, b)= (1.4, 0.05). The solid line is the pruning front. Points represent real orbits.

sequences are leading with the following 32 letters K_f =01 000 101 000 101 000 101 000 101 010 001. An unstable periodic orbits with length $n < 32$ cannot tell the difference between these kneading sequences. Thus, for the unstable periodic orbits with length $n < 32$, the grammar is completely determined by the sequence K_f, that is, a word $S(x)$ corresponds to an unstable periodic orbit of the Hénon map for $(a, b) = (1.4, 0.05)$ if and only if it satisfies

$$\alpha(\sigma^m(S_{\text{forw}}(x))) \leq \alpha(K_f), \quad m = 0, 1, 2, \ldots, \tag{9}$$

where $S_{\text{forw}}(x)$ represents the forward part of $S(x)$. This is just the grammar for a unimodal map with a kneading sequence K_f. Thus, we can say that the topology of the attractor of the Hénon map for $(a, b) = (1.4, 0.05)$ can be approximately represented by that of a unimodal map with a kneading sequence K_f. If the unimodal map is taken as the Logistic map (3), the corresponding value of μ can be determined numerically, which is 1.4715. We have obtained similar results for many other parameters. In Table I, the kneading sequence K_f for $(a, b) = (1.7, 0.01)$ is also presented. The corresponding values of μ for the Logistic map and the fractal dimensions are also listed. The fractal dimensions are computed by a box-counting technique with 10 000 000 points.

The availability of the above grammar means that we can calculate all the periodic orbits up to a definite length. The results are shown in Table II for $a = 1.4$, $b = 0.05$ and $a = 1.7$, $b = 0.01$. The topological entropy K can be calculated for all practical purposes from the rate of increase of the number of allowed periodic points belonging to orbits of length n. Denoting the number by $N(n)$, we have

$$K = \lim_{n \to \infty} \frac{\ln N(n)}{n}. \tag{10}$$

We also have calculated the nth-order approximant of the topological entropy defined by

$$K^{(n)} = \frac{\ln N(n)}{n}. \tag{11}$$

For $a = 1.4$, $b = 0.05$, no orbit with odd period exists except for the repetitions of lower cycles. The nth-order approximant of the topological entropy for even length appears to converge to a value about 0.26. For $a = 1.7$, $b = 0.01$, the nth-order approximant of the topological entropy also seems to converge.

The validity of the above discussion can be checked directly by comparing the unstable periodic orbits from the above grammar with those obtained by the following two techniques. We have calculated all periodic orbits for above two groups of parameters up to length 18 with a Newton procedure. All the symbolic sequences for these periodic orbits are exactly consistent with those calculated by the above grammar. Alternately, the periodic orbits are computed up to length 21 by the techniques of Biham and Wenzel [11]. The numbers of them also exactly agree with those predicted by the above grammar.

From the above discussion, the topology of the attractor of the strongly dissipative Hénon map can be determined by only one kneading sequence to very high

TABLE II. The number of unstable periodic orbits and the nth-order approximant to the topological entropy in the Hénon map for $n > 9$ for $a = 1.4$, $b = 0.05$ and $a = 1.7$, $b = 0.01$. $N_c(n)$ is the number of orbits of length n excluding cyclic permutations and repetitions of lower cycles, $N(n)$ is the total number of periodic orbits of length n and its divisors.

Period	$a = 1.4, b = 0.05$			$a = 1.7, b = 0.01$		
	$N_c(n)$	$N(n)$	$K^{(n)}$	$N_c(n)$	$N(n)$	$K^{(n)}$
10	2	24	0.317805	9	104	0.464439
11	0	2	0.063013	16	178	0.471071
12	2	32	0.288811	21	272	0.467150
13	0	2	0.053319	34	444	0.468910
14	4	60	0.292453	48	704	0.468341
15	0	2	0.04621	72	1092	0.466384
16	5	96	0.285272	110	1792	0.468193
17	0	2	0.040773	166	2824	0.467406
18	8	148	0.277623	248	4552	0.467962
19	0	2	0.036481	380	7222	0.467625
20	11	248	0.275671	571	11528	0.467627
21	0	2	0.033007	874	18384	0.467583
22	18	400	0.272339	1326	29352	0.467596
23	0	2	0.030137	2042	46968	0.467705
24	25	640	0.269227			
25	0	2	0.027726			
26	40	1044	0.267339			
27	0	2	0.025672			
28	58	1688	0.265404			
29	0	2	0.023902			
30	90	2724	0.263662			

accuracy. In practice, the kneading sequence can be calculated from the preimage of the most upper left (the point marked by A in the Fig. 1 which is the point with the minimum x value of the attractor). This allows us to give a very precise and not cumbersome estimate of the characteristic quantities of strange attractors of the strongly dissipative Hénon map.

We can give a geometric explanation for the above observation. For the convenience of the following discussion in this paragraph, we first redefined the partition denoted by P in this paragraph which is the first preimages of the "primary" tangency points [12]. This partition also divides the full phase space into two subsets as shown in Fig. 3. Then the letters 0 and 1 are assigned for the parts left or right to P. In 1987, Gu found that there exists a set of manifolds, called most stable manifolds (MSM's) in 2D space [16, 17]. A MSM is a submanifold in the basin of an attractor such that all the points on this submanifold will converge to a single point with the highest possible exponential rate (i.e., the most negative Lyapunov exponent of the attractor). From this definition, all the (first) images of the points on a MSM must fall on another MSM. Thus, if we take each MSM on a subset as an element, the attractor in 2D space is cut into elements and each element corresponds to a point in a 1D interval. Consequently, the iteration relation between these elements forms a 1D map. In this paper, we call this 1D map the *geometric* 1D *Hénon map*. In Fig. 3, the MSM's for the Hénon map (dashed lines) are also shown. In the following, we will see that this geometric 1D Hénon map is a unimodal one.

For these elements, we can define the ordering rules for them in 2D space. We define right one of two elements to be greater. Consequently, the monotonicity can also be generated for this geometric 1D Hénon map. Numerically, we find the part right to the P has a decreasing monotonicity, whereas that left to the P possesses an increasing monotonicity. Thus, the geometric 1D Hénon

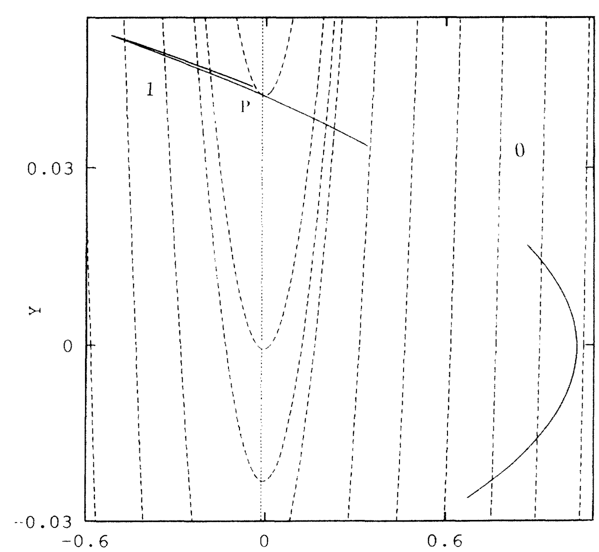

FIG. 3. The strange attractor together with the most stable manifold's (MSM's) of the Hénon map for $(a, b) = (1.4, 0.05)$. The heavy lines are the strange attractor. The dashed lines are part of its MSM's. The dotted line is the partition P for our geometric description of the Hénon map, which also divides the attractor into two parts marked by 0 and 1. The MSM's cut the attractor in each subset into elements. All the points on an elements share a forward symbolic sequence.

map is a unimodal map with a partition P. From the definition of MSM's, the "primary" tangency points are just the tangency points between the attractor and the MSM's. In the strongly dissipative Hénon map, these "primary" tangency points are so close that they can be approximately treated as a single point. Consequently, this point is the maximum of these elements and P is the critical point of this geometric 1D Hénon map.

In fact, the element has close relationship with the symbolic sequence. Since all the points on an element (which is part of an MSM) will converge to a single point, all the points in phase space sharing the same forward sequence must fall on a same element. For the Hénon map with sufficiently small b, we conjecture that all points on an element (on or close to the attractors) sharing one forward word. Numerically, this conjecture can be verified directly by iterating the map (1) from two initial points on an element. Then each element defined above corresponds to a forward symbolic sequence.

It is clear that the symbolic sequence for a trajectory in this way is equal to that of the above 2D representation with only one shift.

Now we consider the Hénon map of a little larger b for $(a,b) = (1.4,\ 0.1)$. The fractal dimension is 1.13 ± 0.02. In Fig. 4 the symbolic plane is shown. The forward parts of all the 20 kneading sequences are leading with $K_f = 010\,000\,000$. It has been checked directly with a Newton procedure that the unstable periodic or-

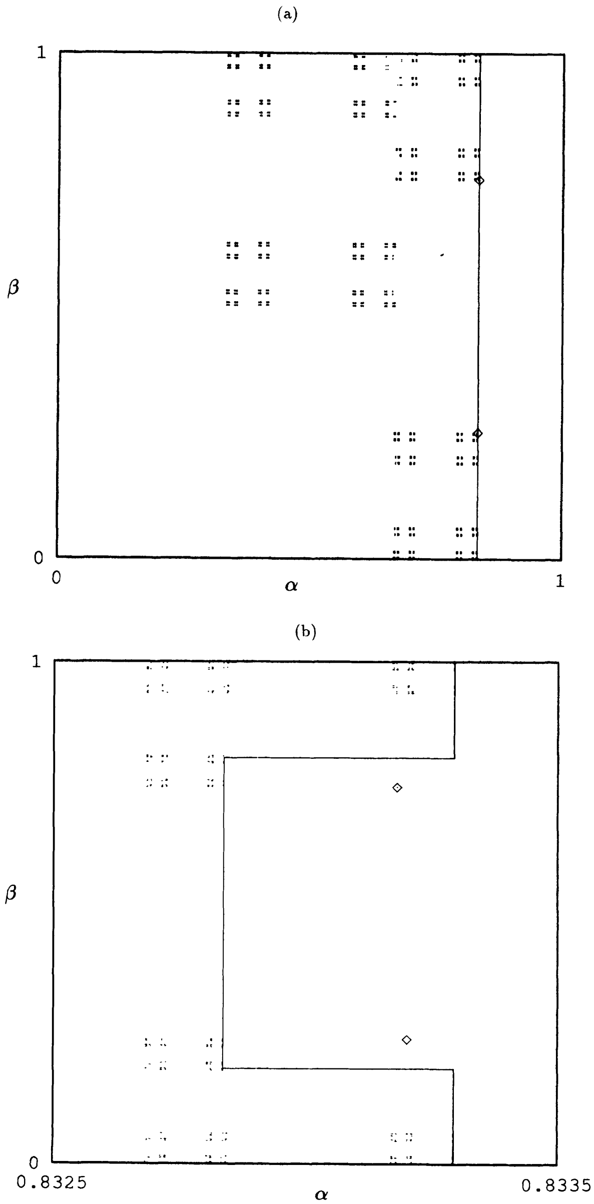

FIG. 4. The symbolic plane of the Hénon map for $(a,b)=$ (1.4, 0.1). The diamonds represent two forbidden points (α $(010^9100\bullet010^9100)$, β $(010^9100\bullet010^9100)$) and ($\alpha$ $(010^9101\bullet010^9101)$, β $(010^9101\bullet010^9101)$); (b) an enlarged part of the symbolic plane.

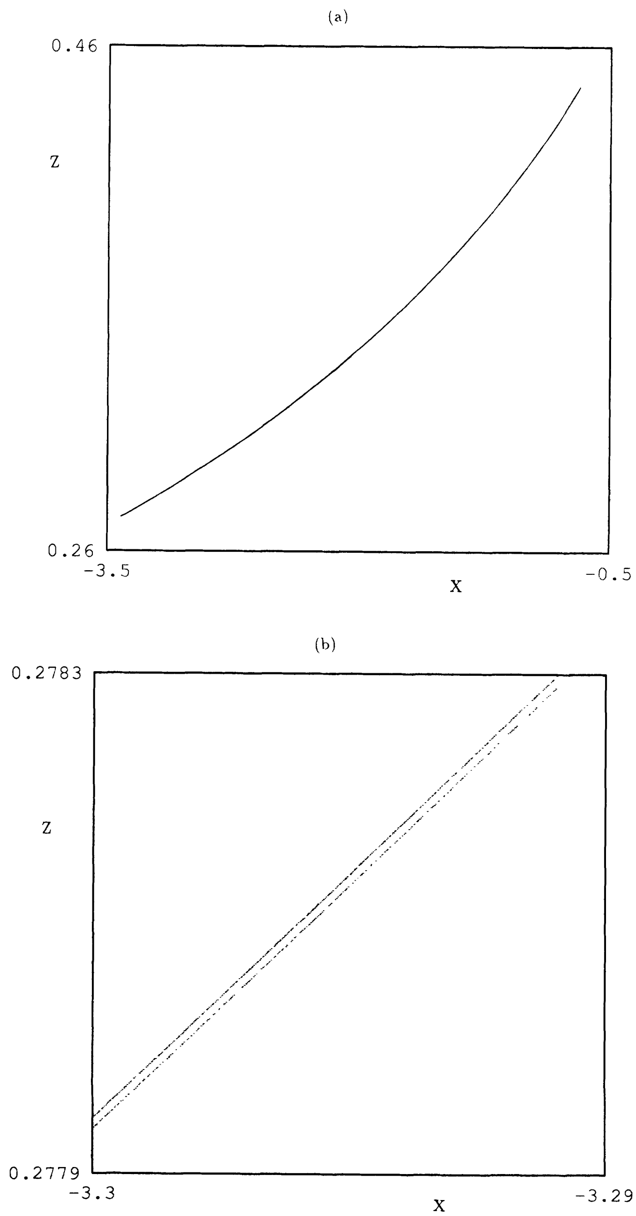

FIG. 5. The 2D attractor of the Rössler band for parameters $c = 2$, $d = 4$ and $a = 0.408$; (b) an enlarged part of the attractor.

bits can be properly generated by the grammar (6) with this K_f up to period 9. Deviations are found for period 14 orbits. Numerically one kneading sequence is determined with its forward part $K_A = 010^{10}01000101$ (see the point A in Fig. 1). With this kneading sequence 19 unstable periodic orbits are allowed in which the words 010^9100 and 010^9101 are not found with a Newton procedure. From the symbolic plane shown in Fig. 4(b), the two points (α ($010^9100\bullet010^9100$), β ($010^9100\bullet010^9100$)) and (α ($010^9101\bullet010^9101$), β ($010^9101\bullet010^9101$)) (diamonds) both fall into the forbidden zone.

IV. THE DYNAMICS OF OTHER HIGH-DIMENSIONAL SYSTEMS

The above idea can be extended to many other systems. Here, we only take the Rössler's band

$$\begin{aligned} \dot{x} &= -y - x\,, \\ \dot{y} &= x + ay\,, \\ \dot{z} &= b + z(x - c)\,, \end{aligned} \tag{12}$$

as an example. The 2D attractor is shown in Fig. 5 for parameters $c = 2$, $d = 4$, and $a = 0.408$. This attractor is cut from the 3D flow on the half plane $y = 0$, $x < 0$. With a box-counting technique, the fractal dimension for the 2D attractor is 1.035± 0.016. The forward part of a kneading sequence is determined numerically, which is K_f = 0 100 100 100 100 010 000 001 001. With a Newton procedure we have computed all unstable periodic orbits up to length 12. The symbolic sequences for them are in exact agreement with those predicted by the grammar (6) with the above kneading sequence K_f.

It should be noted that our idea can be also applied to some dynamical systems with moderate dissipation in some special cases. For the following 2D antisymmetrical map [18]

$$\begin{aligned} x_{n+1} &= Ax_n^3 + (1 - A)x_n + by_n, \\ y_{n+1} &= x_n, \end{aligned} \tag{13}$$

we have found that the topologies for all the symmetry-breaking attractors are close to 1D. The symmetry-breaking attractor for $A = 2.95$ and $b = 0.25$ is shown in Fig. 6. It has been found that all periodic orbits up to length 8 are completely determined with only one kneading sequence.

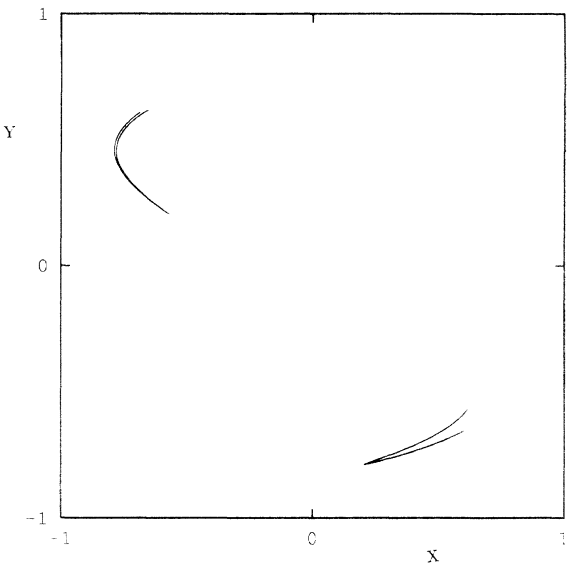

FIG. 6. The symmetry-breaking attractor of the 2D antisymmetrical map (12) for $A = 2.95$ and $b = 0.25$.

V. CONCLUSION

In this paper, we have shown that the $1 + \epsilon$-dimensional attractor of the strongly dissipative Hénon map can be reduced to an effectively 1D one. Extending this idea to many other systems explains the observations that the topology for the attractors on proper Poincáre sections for these systems can be described by a 1D map rather well, and the numerical results that for maps of the annulus of the family (4) there exists a value b_c, such that for $b < b_c$ the topology is identical to that of the circle map. An example for the Rössler band is also presented. With this idea we can give a very precise and not too cumbersome estimate of the characteristic quantities of strange attractors for strongly dissipative dynamical systems. It should be noted that the attractors for dynamical systems with moderate dissipation can also be interpreted as 1D in some special cases.

ACKNOWLEDGMENTS

The author thanks Professor Hao Bai-lin for his encouragement. This work was partially supported by a grant from CNSF, and by the Computer Center of the ITP which provides me with SUN computer workstation time.

[1] M. Hénon, Commun. Math. Phys. **50**, 65 (1976).
[2] G.H. Gunaratne, M.H. Jensen, and I. Procaccia, Nonlinearity **1**, 157 (1988).
[3] M.Z. Ding and B.L. Hao, Commun. Theor. Phys. **9**, 375 (1988); H.P. Fang and B.L. Hao (unpublished).
[4] Y. Ueda, Chaos Solitons Fractals **1**, 199 (1991); Fu Shanqing, M. S. thesis, Institute of Theoretical Physics, P. R. China, 1993.
[5] B.L. Hao, Physica A **104**, 85 (1986).
[6] O. E. Rössler, Phys. Lett. A **57**, 397 (1976).
[7] E. Knobloch, D. R. Moore, J. Toomre, and N. O. Weiss, J. Fluid Mech. **166**, 409 (1986); D. R. Moore and N.

O. Weiss, Philos. Trans. R. Soc. London Ser. A **332**, 121 (1990); M. R. E. Proctor and N. O. Weiss, Nonlinearity **3**, 619 (1990).

[8] G. H. Gunaratne, P. S. Linsay, and M. J. Vinson, Phys. Rev. Lett. **63**, 1 (1989).

[9] R. H. Simoyi, A. Wolf, and H. L. Swinney, Phys. Rev. Lett. **49**, 245 (1982); K. Coffman, W.D. McCormick, and H. L. Swinney, *ibid.* **56**, 999 (1986).

[10] D. Auerbach, P. Cvitanovic, J. P. Echmann, G. H. Gunaratne, and I. Procaccia, Phys. Rev. Lett. **58**, 2387 (1987).

[11] D. Biham and W. Wenzel, Phys. Rev. Lett. **63**, 819 (1989).

[12] P. Grassberger, and H Kantz, Phys. Lett. A **113**, 235 (1985); Physica D **17**, 75 (1985).

[13] Hao Bai-lin, *Elementary Symbolic Dynamics and Chaos in Dissipative Systems* (World Scientific, Singapore, 1989).

[14] G. D'Alessandro, P. Grassberger, S Isola, and A Politi, J. Phys. A **23**, 5295 (1990).

[15] P. Cvitanovic, G. H. Gunaratne, and I. Procaccia, Phys. Rev. A **38**, 1503 (1988).

[16] Y. Gu, Phys. Lett. A **124**, 340 (1987).

[17] H. Zhao and W.M. Zheng, Commun. Theor. Phys. **19**, 21 (1993).

[18] H.P. Fang (unpublished).